

The effect of carotid artery stenting on capillary transit time heterogeneity in patients with carotid artery stenosis

European Stroke Journal
2018, Vol. 3(3) 263–271
© European Stroke Organisation
2018

Article reuse guidelines:
sagepub.com/journals-permissions
DOI: 10.1177/2396987318772686
journals.sagepub.com/home/eso



Ethem M Arsava¹ , Mikkel B Hansen², Berkan Kaplan¹, Ahmet Peker³ , Rahsan Gocmen³, Anil Arat³, Kader K Oguz³, Mehmet A Topcuoglu¹, Leif Østergaard^{2,4} and Turgay Dalkara^{1,5}

Abstract

Introduction: Carotid revascularisation improves haemodynamic compromise in cerebral circulation as an additional benefit to the primary goal of reducing future thromboembolic risk. We determined the effect of carotid artery stenting on cerebral perfusion and oxygenation using a perfusion-weighted MRI algorithm that is based on assessment of capillary transit-time heterogeneity together with other perfusion and metabolism-related metrics.

Patients and methods: A consecutive series of 33 patients were evaluated by dynamic susceptibility contrast perfusion-weighted MRI prior to and within 24 h of the endovascular procedure. The level of relative change induced by stenting, and relationship of these changes with respect to baseline stenosis degree were analysed.

Results: Stenting led to significant increase in cerebral blood flow ($p < 0.001$), and decrease in cerebral blood volume ($p = 0.001$) and mean transit time ($p < 0.001$); this was accompanied by reduction in oxygen extraction fraction ($p < 0.001$) and capillary transit-time heterogeneity ($p < 0.001$), but an overall increase in relative capillary transit-time heterogeneity (RTH: CTH divided by MTT; $p = 0.008$). No significant change was observed with respect to cerebral metabolic rate of oxygen. The median volume of tissue with MTT $> 2s$ decreased from 24 ml to 12 ml ($p = 0.009$), with CTH $> 2s$ from 29 ml to 19 ml ($p = 0.041$), and with RTH < 0.9 from 61 ml to 39 ml ($p = 0.037$) following stenting. These changes were correlated with the baseline degree of stenosis.

Discussion: Stenting improved the moderate stage of haemodynamic compromise at baseline in our cohort. The decreased relative transit-time heterogeneity, which increases following stenting, is probably a reflection of decreased functional capillary density secondary to chronic hypoperfusion induced by the proximal stenosis.

Conclusion: Carotid artery stenting, is not only important for prophylaxis of future vascular events, but also is critical for restoration of microvascular function in the cerebral tissue.

Keywords

Atherosclerosis, carotid artery stenting, perfusion MRI, capillary transit time, flow heterogeneity

Date received: 30 November 2017; accepted: 1 April 2018

Introduction

Atherosclerotic lesions causing moderate to severe stenosis in extracranial carotid arteries constitute a significant contributor of ischaemic strokes in the adult population.¹ Despite the success attained by medical therapies over the last two decades, revascularisation of the stenotic segment, either by endarterectomy or endovascular techniques, still remains a therapeutic option in symptomatic and selected asymptomatic

¹Department of Neurology, Faculty of Medicine, Hacettepe University, Turkey

²Department of Clinical Medicine, Center of Functionally Integrative Neuroscience, Aarhus University, Denmark

³Department of Radiology, Faculty of Medicine, Hacettepe University, Turkey

⁴Department of Neuroradiology, Aarhus University Hospital, Denmark

⁵Institute of Neurological Sciences and Psychiatry, Hacettepe University, Turkey

Corresponding author:

Ethem M Arsava, Department of Neurology, Faculty of Medicine, Hacettepe University, Sıhhiye, Ankara 06100, Turkey.
Email: arsavaem@hotmail.com

patients with moderate to severe carotid artery stenosis.¹ Although the primary goal of revascularisation therapies is to minimise future embolic events originating from atherosclerotic plaques, the improvement of haemodynamic compromise within the distal vascular bed comes forward as a secondary gain, which is considered to play an important role in long-term morbidities associated with carotid atherosclerosis such as the emergence of white matter (WM) lesions and cognitive dysfunction.^{2,3}

A number of studies have explored the influence of carotid revascularisation on cerebral haemodynamics, using methodologies like dynamic susceptibility contrast (DSC)^{4,5} or arterial spin labelling (ASL),^{6,7} perfusion-weighted magnetic resonance imaging (PWI), quantitative magnetic resonance imaging angiography,⁸ Xe-133 based flow assessment techniques,^{9,10} or single photon emission computed tomography.^{11,12} These studies suggest that improvements in cerebral blood flow (CBF) start as early as a few hours following the revascularisation procedure. While the reduction in regional blood supply as a result of the proximal stenosis may limit brain oxygenation, the accompanying changes in distal perfusion pressure may also disturb the haemodynamics across the distal microcirculation, limiting oxygen extraction efficacy.¹³ Now, DSC-PWI methods make it possible to non-invasively estimate both CBF and the microvascular distribution of blood in terms of the so-called capillary transit-time heterogeneity (CTH).^{13–15} Based on these parameters, the effects of both the proximal flow-limiting condition and any distal microvascular disturbance on brain oxygenation can be estimated in terms of regional oxygen extraction fraction (OEF) and cerebral metabolic rate of oxygen (CMRO₂) that can be supported in steady state at normal tissue oxygen tension.^{13–15} In this study, we determined the influence of carotid artery stenting on these perfusion metrics and the corresponding brain oxygenation in a cohort of patients with carotid artery stenosis.

Methods

A total of 41 patients scheduled to undergo stenting for carotid artery stenosis were included into this prospective study, which aimed to investigate the influence of carotid revascularisation on cerebral haemodynamics. All patients underwent magnetic resonance imaging (MRI) before and within 24 h after the endovascular procedure. Of the 41 patients enrolled into the study, eight patients were excluded due to extensive WM hyperintensities and chronic infarcts ($n = 1$), poor perfusion imaging raw data quality ($n = 4$) or contralateral ICA occlusion ($n = 3$). The final study population,

hence, comprised 33 patients. The study was approved by the local institutional review board.

All MRI data were acquired on a 3T scanner (Philips Ingenia, Best, Netherlands). The MRI protocol included T2* gradient-recalled echo (GRE) DSC imaging (TR/TE: 2336/40 ms, 40 dynamic measurements), diffusion-weighted imaging (TR/TE: 2994/94 ms, $b = 0$ and, 1500 s/mm²), T2 fluid-attenuated inversion recovery (T2-FLAIR) imaging (TR/TE/TI: 11000/125/2800 ms) and low flip-angle T1-weighted (T1) imaging (TR/TE; 10/1.95 ms, flip angle: 15°). For DSC imaging, a dose of 0.1 mmol/kg bodyweight Gadolinium (Gd) based contrast media (gadoteric acid) was administered intravenously using a power-injector (OptiStar® Elite MR Contrast Delivery System, Mallinckrodt Pharmaceuticals, Hazelwood, MO) at a rate of 5 ml/s followed by 20-ml saline tracer injected at the same rate.

Image processing

Each perfusion series was motion corrected through 12-parameter affine registration of all 3D image volumes in the series to the first acquisition volume using a normalised mutual information (NMI) cost function. Next, a suitable arterial input function (AIF) was obtained automatically¹⁶ from a region of interest (ROI) drawn on the motion corrected 4D image volume (three spatial dimensions and time) in the MCA territory contralateral to the stenotic side. Subsequently, the motion-corrected perfusion data were spatially smoothed using a 3 × 3 uniform kernel for each 2D slice and the intensity data converted into contrast media concentration-time curves (CTCs) for each voxel k

$$CTC_k(t) = -\frac{1}{r_2 T_E} \ln\left(\frac{S_k(t)}{S_k(0)}\right)$$

where t denotes time, r_2 is a constant known as the T2*-relaxivity of the contrast media, T_E the echo time and $S_k(t)$ the observed MRI signal intensity for voxel k at time t . We assume a linear relationship between Gadolinium concentration and signal change,^{17,18} i.e.

$$R2^*(t) = R2_0^* + r_2[Gd](t)$$

where $[Gd](t)$ denotes the concentration of Gd-containing contrast agent at time t .

From the individual CTC's, haemodynamic markers were subsequently calculated by a parametric Bayesian deconvolution algorithm,^{14,15} which generates traditional haemodynamic markers such as CBF and – volume (CBV), mean transit time (MTT), delay

between site of measurement of the AIF and site of measurement of the CTCs, as well as capillary transit-time heterogeneity (CTH), relative CTH (RTH: CTH divided by MTT). Based on these, OEF and CMRO₂ are then calculated.¹³ Perfusion data processing was performed using the PGUI software (<http://cfin.au.dk/software/pgui>), except for the motion correction, where the statistical parametric mapping toolbox version 12 (SPM12) was used.

Grey matter (GM), WM and cerebrospinal fluid (CSF) masks were produced from the T1-weighted images using the automated unified segmentation method¹⁹ implemented in SPM12. T2-hyperintense lesions including subacute ischaemic lesions, chronic infarcts and WM hyper-intensities were manually outlined on T2-FLAIR images by an experienced neurologist (EMA). Both the T1 and T2-FLAIR images, and their associated masks, were subsequently registered to the pre-stenting GRE-DSC space using SPM12.

To limit the analyses to the affected vascular territory, a generic middle cerebral artery (MCA) mask was obtained from Tatu et al.²⁰ and registered to the pre-stenting T1 image from one of the patients. Subsequently, this mask was manually adjusted to yield an MCA territory mask in the known T1 image space. This procedure allowed for the subsequent registration of the MCA mask to GRE-DSC space through the registration of the MCA reference T1 image to the T1 images in GRE-DSC space.

Finally, post-stenting GRE-DSC images and maps were registered to the pre-stenting GRE-DSC space, resulting in all images, maps and masks being transformed to the same space.

ROI analysis

Based on the image processing steps above, we could extract haemodynamic and metabolic indices for: (i) ipsilateral WM within the MCA territory, (ii) ipsilateral GM within the MCA territory and (iii) combined ipsilateral WM and GM within the MCA territory. All extracted values were normalised to the average value within the corresponding contralateral MCA mask from which tissue annotated as T2-FLAIR hyper-intensities was excluded. Normalisation was performed by division with the contralateral average for CBV, CBF and CMRO₂ values, while the contralateral average was subtracted during normalisation of MTT, CTH, delay, OEF and RTH values.

The same semi-automatically generated MCA territory masks were used in conjunction with thresholding to provide volumetric estimates of the extent of pre- and post-stenting hypo-perfusion, thus providing an overall idea of the extent of normalisation of the perfusion deficit. The values that best differentiated

ipsi- and contralateral MCA regions on pre-stent images according to receiver operating characteristics curve analyses were chosen as the thresholds used in this analysis.

Statistical analysis

Categorical variables are expressed as number of positive subjects (n) and the corresponding percentage of the study population (%), while continuous variables are presented as median values and associated interquartile range (IQR). The significance of the median change in the normalised perfusion parameters in GM, WM and the entire territory from pre- to post-stenting time points was tested by the use of Wilcoxon signed rank test. Correlation analyses were performed by Spearman's test. A *p* value of <0.05 was considered statistically significant. Statistical analyses were performed by SPSS 16.0.

Results

The study population comprised 12 female and 21 male patients with a median (IQR) age of 66 (61–73) years. The median (IQR) residual luminal diameter at the stenotic site was 1.00 (0.70–1.4) mm leading to an overall 76 (68–84) % stenosis (according to the NASCET criteria²¹). Carotid artery stenting was performed after a median (IQR) duration of 3 (2–11) weeks following the stroke, among the 25 patients with symptomatic stenosis. The procedure resulted in new ischaemic lesions on DWI in eight (24%) patients, none of them being symptomatic. Further characteristics of the study population are summarised in Table 1. The clinical features of the study cohort were similar to those of patients excluded from the study.

In Figure 1, we present examples of four patients treated with stenting for carotid artery stenosis. The images display, for each subject, pre-stenting T1, T2-FLAIR, and CTH images, post-stenting CTH image, and the generated MCA, WM, GM, and

Table 1. Clinical and imaging characteristics of the study population.

Risk factors (n, %)	
Hypertension	25 (76%)
Diabetes mellitus	16 (49%)
Hyperlipidemia	17 (52%)
Coronary artery disease	14 (42%)
Smoking	6 (18%)
Symptomatic carotid artery stenosis (n, %)	25 (76%)
Duration between stenting and follow-up MRI (median, IQR)	16 (8–22) h

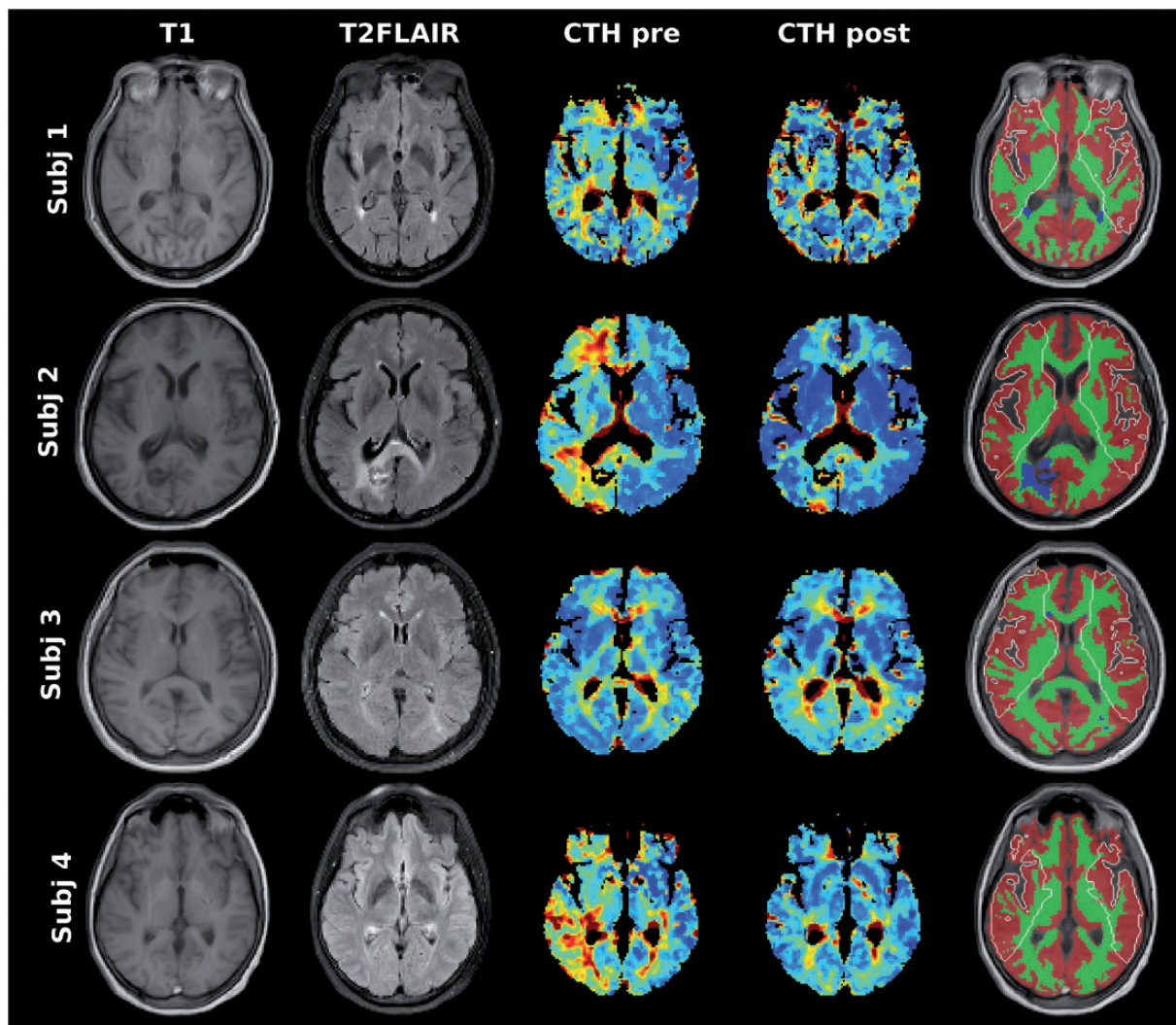


Figure 1. Illustration of images and annotations for four subjects with carotid stenosis undergoing stenting (Subject 1: Male, 52 years old, 51% right-sided stenosis; Subject 2: Female, 59 years old, 79% right-sided stenosis; Subject 3: Female, 61 years old, 63% left-sided stenosis; Subject 4: Female, 57 years old, 78% right-sided stenosis). The green, red, and blue annotations correspond to WM, GM, and WM hyperintensity regions, respectively, while the white contour denotes the MCA territory.

T2-FLAIR hyper-intensity masks overlaid on the pre-stenting T1 image. Subjects 2 and 4, and to a lesser extent subject 1, all with right sided carotid artery stenosis, display reduction of CTH in the affected hemisphere following the procedure, thereby resulting in normalisation of CTH compared to the unaffected hemisphere. The effect of the procedure for subject 3 (left sided stenosis) appears to be less pronounced. These patterns seem to match reasonably well with the stenosis degrees (see below for details), where the stenosis degrees for subjects 2 (79%) and 4 (78%) are substantially larger than for subjects 1 (51%) and 3 (63%).

Compared to baseline imaging, carotid artery stenting led to a significant increase in CBF, together with a decrease in CBV and MTT in the ipsilateral MCA

territory (Table 2, Figures 2 and 3). In our population analyses, this was accompanied by a significant decrease in CTH; with the parallel decrease in MTT stenting resulted in an overall increase in RTH. The normalisation of the circulation led to a reduction of OEF, but no significant change in CMRO₂. All changes were similar when the flow haemodynamics were examined separately in the GM and WM (Table 2), when the group was stratified according the presence or absence of procedure-related new ischaemic lesions, and the entire MCA territory was examined without extraction of T2-FLAIR hyperintensities from the masks. The median (IQR) volume of tissue with MTT > 2s decreased from 24 (13–43) ml to 12 (7–21) ml ($p=0.009$), with CTH > 2s from

Table 2. The direction and significance of change promoted by stenting on imaging variables.

		Entire territory	White matter	Grey matter
CBV	↓	0.001	<0.001	0.001
CBF	↑	<0.001	<0.001	<0.001
MTT	↓	<0.001	<0.001	<0.001
Delay	↓	<0.001	<0.001	<0.001
CTH	↓	<0.001	0.001	<0.001
RTH	↑	0.008	0.004	0.013
OEF	↓	<0.001	<0.001	<0.001
CMRO ₂	–	0.127	0.110	0.208

CBV: cerebral blood volume; CBF: cerebral blood flow; MTT: mean transit time; CTH: capillary transit-time heterogeneity; RTH: relative transit-time heterogeneity; OEF: oxygen extraction fraction; CMRO₂: cerebral metabolic rate of oxygen.

29 (16–44) ml to 19 (10–32) ml ($p=0.041$) and with RTH < 0.9 from 61 (32–108) ml to 39 (26–70) ml ($p=0.037$) following the stenting procedure. The post-procedural CBF in the ipsilateral hemisphere was greater than the contralateral side in 10 patients (30%); the degree of baseline stenosis was significantly higher among these cases [85% (78–86) vs. 74% (63–79); $p=0.007$]. Two of these patients developed hyperperfusion syndrome clinically during follow-up; nonetheless, we were not able to identify a specific imaging signature that could be predictive of this syndrome.

The degree of stenosis was moderately, but significantly, correlated with all baseline imaging parameters, except for RTH and CMRO₂ [CBV ($r=0.53$; $p=0.001$), CBF ($r=-0.51$; $p=0.003$), MTT ($r=0.58$; $p<0.001$), delay ($r=0.62$; $p<0.001$),

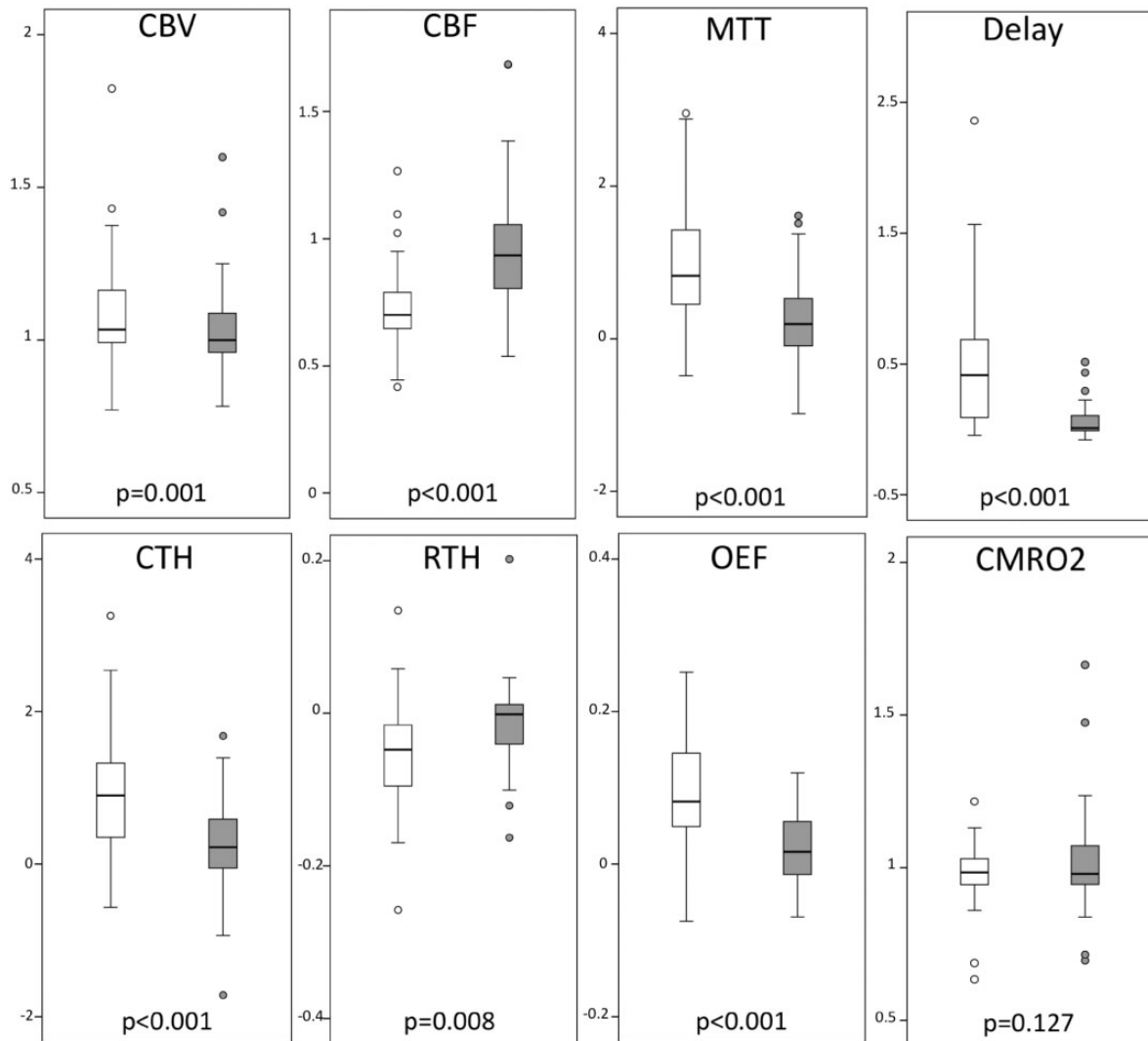


Figure 2. Box-plots of haemodynamic markers prior to (white) and following (grey) carotid artery stenting. For better visualisation of the box-plots, outliers outside the visualisation area are not included in the plots, but are naturally included in the statistical analyses. The y-axes represent the relative values with respect to the contralateral hemisphere.

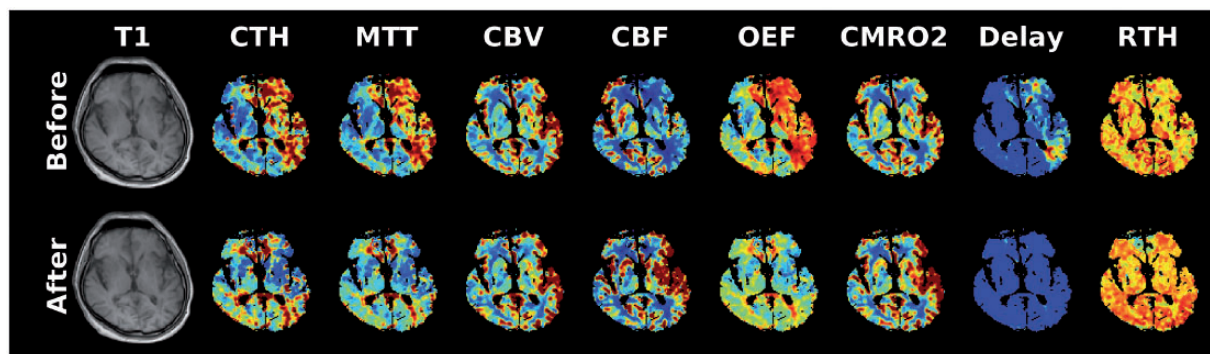


Figure 3. Pre- and post-stent sample images of a patient undergoing left-sided carotid artery stenting.

CTH ($r = 0.59$; $p < 0.001$), OEF ($r = 0.62$; $p < 0.001$]. The degree of improvement introduced by stenting was correlated with the baseline stenosis degree for CBF ($r = 0.57$; $p = 0.001$), MTT ($r = -0.48$; $p = 0.005$), delay ($r = -0.63$; $p < 0.001$), CTH ($r = -0.37$; $p = 0.033$), RTH ($r = 0.35$, $p = 0.044$) and OEF ($r = -0.62$; $p < 0.001$).

Discussion

Similar to previous reports,^{4–12} our study shows that carotid artery stenting improves CBF in the distal territory. As a novel observation, we have shown that this improvement was accompanied by a decrease in the overall capillary transit time heterogeneity, but increase in relative heterogeneity, and normalisation of the increased OEF. Notably, no significant CMRO₂ changes were observed, indicating that brain oxygenation remained coupled to the metabolic needs of the tissue throughout the course of the treatment, despite the changes in the haemodynamic status. Although the latter could be comforting at first look, the risks posed by alterations in capillary dysfunction could be significant before and right after revascularisation. The present cohort is too small to identify these potential clinical implications in the setting of carotid stenosis, like cognitive decline if untreated or hyperperfusion syndrome if treated, but assessment of the capillary function appears to be a promising MRI tool in this regard.

The baseline haemodynamic characteristics detected in our cohort suggest that these patients were in a moderate stage (stage II²²) of haemodynamic compromise, where CBF decrease was accompanied by an elevation in CBV and OEF. Expectedly, the level of haemodynamic compromise was more pronounced in the group of patients with higher degree of stenosis, as was the improvement observed following stenting. Although blood supply is a very important component of cerebral haemodynamics, recent studies have suggested that the distribution of flow in the capillaries is critical for efficient oxygen extraction by the cerebral tissue.¹³

This heterogeneity has been shown to adversely influence outcome in acute stroke,^{14,23} and to correlate with the extent of cognitive decline in conditions suspected to cause capillary dysfunction, such as Alzheimer's disease.²⁴ Our study, consistent with previous observations in patients with bilateral carotid artery disease,²⁵ suggests that proximal stenosis leads to an increased heterogeneity in capillary transit time (CTH) in addition to disturbances in CBF. Importantly, this heterogeneity can be partially reversed by revascularisation treatments, such as stenting. In passive, compliant microvascular networks, the CTH to MTT ratio is expected to remain constant as blood flow changes.²⁶ While both MTT and CTH decreased after revascularisation, the parallel increase in RTH – the CTH:MTT ratio – indicates that CTH and MTT responses differed from those expected in a normal microcirculation following an increase in blood flow, thereby suggesting an unequal response of bulk flow (through the MTT parameter) and microvascular flow distribution (through the CTH parameter). Several phenomena might explain this finding. First, a relative homogenisation of capillary flow patterns has previously been reported by Hudetz et al.²⁷ in conditions of reduced cerebral perfusion pressure. The lower pre-recanalisation RTH values could thus reflect compensatory homogenisation of transit times to improve oxygen extraction under conditions of impaired perfusion pressure. Pre-recanalisation RTH did not, however, correlate with the degree of stenosis, as one would then have expected. A second explanation for the reduced pre-recanalisation RTH could be the presence of occluded capillaries, as recently shown in acute ischaemic stroke.^{14,28} In a mouse model of chronic hypoperfusion, Srinivasan et al.²⁹ showed that the density of perfused capillaries decreases in proportion to the reduction in CBF, reaching as many as 25% erythrocyte-free capillaries for blood flows well above the ischaemic threshold. In a similar model, Yata et al.³⁰ detected minute-long plugging of a significant

proportion of deep cortical capillaries by leukocytes and ascribed this to adhesion of activated leukocytes to the capillary endothelium via surface receptors (selectins). Unlike our earlier findings in stroke,²⁸ reduced RTH was not accompanied by reduced CBV in hypoperfused tissue in the present study, in fact quite the opposite. Keeping in mind that we measured CBV by a tracer that distributes in the plasma space, our findings are, however, consistent with temporary capillary occlusions by leukocytes, and capillary constrictions that allow plasma but not erythrocytes to pass. In both cases, transit times would tend to homogenise in the normally perfused capillaries without reducing CBV, which we would infer from our measurements.

Although our study is primarily a proof of concept study highlighting the use of microvascular transit-time heterogeneity imaging in the peri-revascularisation setting, it might have potential implications from the clinical point of view. Apart from thromboembolic complications, one other important consequence of carotid atherosclerotic lesions is cognitive decline.^{31,32} The exact nature of this relationship is not known; yet, cerebral hypoperfusion is considered as a factor contributing to long-term cognitive decline.³² The answer to the important question of whether this negative influence on cognitive function can be restored by revascularisation therapies remains unsettled. There are studies that suggest both benefit or harm of endarterectomy or stenting on cognitive tests following the procedure.³² The presence of versatile tissue characteristics, both in terms of haemodynamics and metabolism, and the resulting inevitable heterogeneity among studies could have contributed to these conflicting observations in the literature. It should be kept in mind that cerebral capillary function is affected by the same risk factors as those that predisposed our patients to develop carotid stenosis. Accordingly, risk factors, such as hypertension, diabetes, smoking and hyperlipidemia, are known to alter the morphology of the capillary basement membrane, the integrity of the protective glycocalyx that covers endothelial cells and the viscosity of blood.³³ In particular, glycocalyx damage exposes endothelial adhesion molecules and initiates leukocyte rolling. Hence, the decreased RTH at baseline in relative terms (with respect to the contralateral MCA territory) distal to the stenotic side should not imply the presence of a normal microvascular architecture in our patients. The decrease in the density of perfused capillaries and presence of capillary leukocyte pluggings shown in experimental models of chronic cerebral hypoperfusion could have contributed to the observed pseudo-homogenisation in capillary transit time.^{29,30} Capillary rarefaction is detected as one of the initial manifestations of microvascular dysfunction not only in chronic cerebral hypoperfusion, but also in

a wide spectrum of cerebral disorders.^{34,35} The restoration of disturbed haemodynamics to a certain extent by revascularisation suggests that this rarefaction was functional, rather than structural in our patients. Still, functional microvascular dysfunction is considered as a predecessor of irreversible structural changes,³⁶ and despite therapeutic efforts, patients might still be prone to develop cognitive decline due to persisting changes and deteriorating capillary function, culminating in structural loss of capillaries.³³

Our study discloses that carotid artery stenting, apart from its established efficacy in prophylaxis of future vascular events, is also critical for restoration of microvascular function in the cerebral tissue secondary to stenosis within the proximal arterial tree. As mentioned above, the low number of subjects included represents a limitation of the generalisability of the study. We had to exclude four patients due to poor imaging quality, yet the similarity of clinical characteristics between the excluded cases and study cohort, is suggestive against a potential selection bias. As our study only included patients undergoing carotid artery stenting, our findings need to be replicated in endarterectomy cohorts to suggest that the observed haemodynamic alterations are not restricted to stenting procedures, but rather imply a change as part of carotid revascularisation strategies in general. Of note, we only evaluated changes in cerebral perfusion and metabolism within the initial 24 h following stenting; it therefore remains for forthcoming studies to see how these changes evolve over the following days and affect cerebral haemodynamics in the long run. In conclusion, the clinical implications of the changes in capillary transit time heterogeneity in the setting of carotid stenosis are currently unknown. Future studies could utilise spin-echo DSC MRI to weight CBV and CTH estimates towards the capillary blood compartment³⁷ to determine the influence of capillary function on various aspects of the problem such as cognitive decline, WM lesions or emboli washout,³⁸ and assess the potential of capillary function as a global, therapeutic target in these patients. In this regard, imaging modalities like capillary transit time heterogeneity MRI are not only crucial in understanding microcirculatory dynamics during acute or chronic stages of stroke, but are also promising tools in teasing out the role of capillary function in a vast spectrum of vascular and neurodegenerative cerebral pathologies, where we now realise capillary homeostasis is a key player of the pathophysiology.

Declaration of Conflicting Interests

The author(s) declared the following potential conflicts of interest with respect to the research, authorship, and/or

publication of this article: EMA has received speaker honoraria from Bayer Healthcare, Pfizer, Abbott and Nutricia. He has served on scientific advisory boards for Pfizer, Boehringer Ingelheim, and Nutricia.

MAT has received speaker honoraria from Abbott and Boehringer Ingelheim. He has served on scientific advisory boards for Boehringer Ingelheim. MBH is co-applicant on a patent application based on the presented technique (EP 13185195.8). MBH is a shareholder in Cercare Medical ApS.

Funding

The author(s) disclosed receipt of the following financial support for the research, authorship, and/or publication of this article: The study was funded by the Turkish Academy of Sciences Young Scientists Award Program (GEBIP) awarded to Arsava.

Informed consent

Obtained.

Ethical approval

The study was approved by the Hacettepe University institutional review board.

Guarantor


EMA.

Contributorship

EMA, MBH, MAT, LØ and TD conceived and designed the study. EMA, BK, AP, RG, AA, KKO and MAT acquired clinical and imaging data. MBH performed image processing and analysis. EMA and MBH performed statistical analysis. EMA, MBH, BK, AP, RG, AA, KKO, MAT, LØ and TD contributed to the interpretation of results. EMA and MBH drafted the manuscript. MAT, LØ and TD provided critical revision to the manuscript. All authors reviewed and edited the manuscript and approved the final version of the manuscript.

ORCID iD

Ethem M Arsava  <http://orcid.org/0000-0002-6527-4139>

Ahmet Peker  <http://orcid.org/0000-0002-5998-1304>

References

- Abbott AL, Paraskevas KI, Kakkos SK, et al. Systematic review of guidelines for the management of asymptomatic and symptomatic carotid stenosis. *Stroke* 2015; 46: 3288–3301.
- Buratti L, Viticchi G, Falsetti L, et al. Thresholds of impaired cerebral hemodynamics that predict short-term cognitive decline in asymptomatic carotid stenosis. *J Cereb Blood Flow Metab* 2016; 36: 1804–1812.
- Turk M, Zupan M, Zaletel M, et al. Carotid arterial hemodynamic in ischemic levkoaraiosis suggests hypoperfusion mechanism. *Eur Neurol* 2015; 73: 310–315.
- Wilkinson ID, Griffiths PD, Hoggard N, et al. Short-term changes in cerebral microhemodynamics after carotid stenting. *AJNR Am J Neuroradiol* 2003; 24: 1501–1507.
- Gauvrit JY, Delmaire C, Henon H, et al. Diffusion/perfusion-weighted magnetic resonance imaging after carotid angioplasty and stenting. *J Neurol* 2004; 251: 1060–1067.
- Ances BM, McGarvey ML, Abrahams JM, et al. Continuous arterial spin labeled perfusion magnetic resonance imaging in patients before and after carotid endarterectomy. *J Neuroimaging* 2004; 14: 133–138.
- Yun TJ, Sohn CH, Han MH, et al. Effect of carotid artery stenting on cerebral blood flow: evaluation of hemodynamic changes using arterial spin labeling. *Neuroradiology* 2013; 55: 271–281.
- Shakur SF, Amin-Hanjani S, Bednarski C, et al. Intracranial blood flow changes after extracranial carotid artery stenting. *Neurosurgery* 2015; 76: 330–336.
- Bishop CC, Butler L, Hunt T, et al. Effect of carotid endarterectomy on cerebral blood flow and its response to hypercapnia. *Br J Surg* 1987; 74: 994–996.
- Ko NU, Achrol AS, Martin AJ, et al. Magnetic resonance perfusion tracks 133Xe cerebral blood flow changes after carotid stenting. *Stroke* 2005; 36: 676–678.
- Kojima D, Ogasawara K, Kobayashi M, et al. Effects of uncomplicated carotid endarterectomy on cognitive function and brain perfusion in patients with unilateral asymptomatic severe stenosis of the internal carotid artery by comparison with unoperated patients. *Neurol Res* 2016; 38: 580–586.
- Lishmanov Y, Shvera I, Ussov W, et al. The effect of carotid endarterectomy on cerebral blood flow and cerebral blood volume studied by SPECT. *J Neuroradiol* 1997; 24: 155–162.
- Jespersen SN and Ostergaard L. The roles of cerebral blood flow, capillary transit time heterogeneity, and oxygen tension in brain oxygenation and metabolism. *J Cereb Blood Flow Metab* 2012; 32: 264–277.
- Mouridsen K, Hansen MB, Ostergaard L, et al. Reliable estimation of capillary transit time distributions using DSC-MRI. *J Cereb Blood Flow Metab* 2014; 34: 1511–1521.
- Mouridsen K, Friston K, Hjort N, et al. Bayesian estimation of cerebral perfusion using a physiological model of microvasculature. *Neuroimage* 2006; 33: 570–579.
- Mouridsen K, Christensen S, Gyldensted L, et al. Automatic selection of arterial input function using cluster analysis. *Magn Reson Med* 2006; 55: 524–531.
- Weisskoff RM, Zuo CS, Boxerman JL, et al. Microscopic susceptibility variation and transverse relaxation – theory and experiment. *Magn Reson Med* 1994; 31: 601–610.
- Villringer A, Rosen BR, Belliveau JW, et al. Dynamic imaging with lanthanide chelates in normal brain – contrast due to magnetic-susceptibility effects. *Magn Reson Med* 1988; 6: 164–174.
- Ashburner J and Friston KJ. Unified segmentation. *Neuroimage* 2005; 26: 839–851.
- Tatu L, Moulin T, Bogousslavsky J, et al. Arterial territories of the human brain – cerebral hemispheres. *Neurology* 1998; 50: 1699–1708.

21. North American Symptomatic Carotid Endarterectomy Trial Collaborators, Barnett HJM, Taylor DW, Haynes RB, et al. Beneficial effect of carotid endarterectomy in symptomatic patients with high-grade carotid stenosis. *N Engl J Med* 1991; 325: 445–453.
22. Nemoto EM, Yonas H, Kuwabara H, et al. Identification of hemodynamic compromise by cerebrovascular reserve and oxygen extraction fraction in occlusive vascular disease. *J Cereb Blood Flow Metab* 2004; 24: 1081–1089.
23. Østergaard L, Jespersen SN, Mouridsen K, et al. The role of the cerebral capillaries in acute ischemic stroke: the extended penumbra model. *J Cereb Blood Flow Metab* 2013; 33: 635–648.
24. Nielsen RB, Egefjord L, Angleys H, et al. Capillary dysfunction is associated with symptom severity and neurodegeneration in Alzheimer's disease. *Alzheimers Dement* 2017; 13: 1143–1153.
25. Mundiyanapurath S, Ringleb PA, Diatschuk S, et al. Capillary transit time heterogeneity is associated with modified Rankin scale score at discharge in patients with bilateral high grade internal carotid artery stenosis. *PLoS One* 2016; 11: e0158148.
26. Rasmussen PM, Jespersen SN and Østergaard L. The effects of transit time heterogeneity on brain oxygenation during rest and functional activation. *J Cereb Blood Flow Metab* 2015; 35: 432–442.
27. Hudetz AG, Fehér G and Kampine JP. Heterogeneous autoregulation of cerebrocortical capillary flow: evidence for functional thoroughfare channels? *Microvasc Res* 1996; 51: 131–136.
28. Engedal TS, Hjort N, Hougaard KD, et al. Transit time homogenization in ischemic stroke – a novel biomarker of penumbral microvascular failure? *J Cereb Blood Flow Metab*. Epub ahead of print 1 January 2017. DOI: 10.1177/0271678X17721666.
29. Srinivasan VJ, Yu E, Radhakrishnan H, et al. Microheterogeneity of flow in a mouse model of chronic cerebral hypoperfusion revealed by longitudinal Doppler optical coherence tomography and angiography. *J Cereb Blood Flow Metab* 2015; 35: 1552–1560.
30. Yata K, Nishimura Y, Unekawa M, et al. In vivo imaging of the mouse neurovascular unit under chronic cerebral hypoperfusion. *Stroke* 2014; 45: 3698–3703.
31. Bakker FC, Klijn CJ, Jennekens-Schinkel A, et al. Cognitive disorders in patients with occlusive disease of the carotid artery: a systematic review of the literature. *J Neurol* 2000; 247: 669–676.
32. Wang T, Mei B and Zhang J. Atherosclerotic carotid stenosis and cognitive function. *Clin Neurol Neurosurg* 2016; 146: 64–70.
33. Østergaard L, Engedal TS, Moreton F, et al. Cerebral small vessel disease: capillary pathways to stroke and cognitive decline. *J Cereb Blood Flow Metab* 2016; 36: 302–325.
34. Joutel A, Monet-Leprêtre M, Gosele C, et al. Cerebrovascular dysfunction and microcirculation rarefaction precede white matter lesions in a mouse genetic model of cerebral ischemic small vessel disease. *J Clin Invest* 2010; 120: 433–445.
35. Warrington JP, Ashpole N, Csiszar A, et al. Whole brain radiation-induced vascular cognitive impairment: mechanisms and implications. *J Vasc Res* 2013; 50: 445–457.
36. Cheng C, Diamond JJ and Falkner B. Functional capillary rarefaction in mild blood pressure elevation. *Clin Translational Sci* 2008; 1: 75–79.
37. Kjølby BF, Østergaard L and Kiselev VG. Theoretical model of intravascular paramagnetic tracers effect on tissue relaxation. *Magn Reson Med* 2006; 56: 187–197.
38. Caplan LR and Hennerici M. Impaired clearance of emboli (washout) is an important link between hypoperfusion, embolism, and ischemic stroke. *Arch Neurol* 1998; 55: 1475–1482.